

Two Morphologically Different Mitochondrial Populations in the Rat Hepatocyte as Determined by Quantitative Three-Dimensional Electron Microscopy¹

E. R. BERGER

Special Research Laboratory for Oral Tissue Metabolism, Veterans Administration Hospital, Brooklyn, New York 11209

Received February 22, 1972, and in revised form March 20, 1973

Applying the Sjöstrand technique of making three-dimensional reconstructions from serial thin sections for electron microscopy, it has been determined that rat liver mitochondria lack morphological homogeneity. Nearly 900 mitochondria from three hepatocytes of two specimens were analyzed. Within single cells there are two mitochondrial populations: rod- and V-shapes in a two-to-one ratio. Each population seems to be arrayed in the size gradient between the central vein and hepatic arteriole that has been established by Loud. The data suggest that the mitochondrial numbers vary so as to maintain relatively constant mitochondrial volume per cytoplasmic volume within the gradient. The present findings possibly allow new interpretations of other enzymological, cell fractionation, and zonal centrifugation data.

For decades isolated rat liver mitochondria commonly have been used as the starting materials for biochemical and enzymological studies. Implicitly it has been assumed that the hepatic mitochondrial population is homogeneous. That electron microscopic examination of mitochondrial fractions revealed mainly circular profiles of rather different fine structure than those seen *in situ* was thought merely to be owing to isolation artifacts. In tissue thin sections there are a variety of profile shapes. Only a pleomorphic model could account for this variety in homogeneous population.

Mitochondrial sizes, numbers, distribution, internal fine structure, biochemistry, and enzyme activities have long been known to be tissue specific. Even within the same tissue, a mitochondrial size gradient (14) has been morphometrically confirmed for liver in an elegant study by Loud (13). Indeed, within the single cell, the neonatal fish photoreceptor, the mitochondria are arrayed in a linear size gradient. The gradient is maturational, however, as they appear to be homogeneous in the adult condition (2). In the sea urchin ovum, rod-shaped mitochondria are found in size classes (3) as a function of their DNA content (4; Berger and Picó, in preparation).

¹ For Doctor M. L. Littman, *requiescat in pace*.

Variations in sizes and volumes of mitochondria within a single cell need not suggest enzymatic heterogeneity. However, recent statistical evidence does indicate a heterogeneous distribution of mitochondrial enzymes in rat liver (25, 26).

In the present study, rat liver mitochondria are reconstructed three-dimensionally from serial thin sections for electron microscopy. Quantitative stereomorphological analysis reveals two radically different mitochondrial populations, small rods, and larger V shapes, within single hepatocytes. A morphometric treatment of other data is consistent with the model of two and probably only two mitochondrial populations.¹

MATERIALS AND METHODS

Tiny pieces of rat liver, about 1 mm³, were quickly dissected, in less than 1 minute following decapitation, and prefixed in isosmolar 2.5% glutaraldehyde (15) buffered at pH 7 with 0.1 M cacodylate for 15 minutes (3×5 minutes) at room temperature. The tissues were in buffered 1% osmium tetroxide made isomolar with sucrose 1 hour at 4°C. Washing after prefixation and osmication was achieved in cold isosmolar buffer. Rapid dehydration followed in an acetone gradient. A Vestopal gradient followed by many changes in pure Vestopal (15) over a 24 hour period allowed infiltration. The blocks were polymerized at 60°C but removed prematurely after 1 day for trimming and then postpolymerized another day.

Large face and serial thin sections were cut with glass knives on an LKB-III Ultrotome after the modified (2) Sjöstrand (19) technique, and the ribbons were supported on carbonized Formvar films spanning Sjöstrand keyholes. The carbon is evaporated on the side of the film to face the beam while the sections are on the opposite side. This is done to protect the sections from beam damage as much as possible. It is inherent in the technique of three-dimensional reconstructions from serial sections that the sections be exposed to the beam over long periods of time relative to conventional microscopy. Time is needed to survey and locate recognizable landmarks, and many plates are exposed from the same sectional area for montage assemblage. The sections were double stained in uranyl acetate (5) and lead citrate (27). Two ribbons of 47 and 40 continuous serial sections (ss), respectively, were cut at a 300 Å setting from the same specimen, designated L13 ss(47) and L13 ss(40) in order to determine the precision of the technique. One ribbon of 26 continuous serial sections was cut at a 500 Å setting from another specimen, L14 ss(26), to determine the accuracy of the results. Specimen L15 was used for mitochondrial size gradient analysis.

An Hitachi HS-8 electron microscope was used. Each plate set included a magnification calibration grating replica² with 882 nm spacing. A field comprising four plates including an easily identifiable landmark was selected and photographed in each serial section.

The calibration plate was printed along with the micrographs on Agfa 11 × 14 inch paper. The four prints comprising each field were assembled into montage employing mapping technique, pinking shears, and Scotch Magic Tape so as to reduce the seam effect. Factors contributing to magnification errors must be carefully controlled for closeness of fit and

¹ Presented in part before the American Society for Cell Biology, New Orleans, 1971: "Two morphologically different mitochondrial populations in rat liver"; and the Biophysical Society, Toronto, 1972: "Two and only two mitochondrial shapes in the rat hepatocyte."

² Ernest F. Fullam, Inc., Schenectady, New York.

reliable measurements. Therefore each operation, i.e., microscopy, printing, washing, and drying, must be completed in the same time period and all the micrographs including calibration handled together.

The mitochondrial profiles were traced from the montages with india ink onto 11×14 inch plastic transparent sheets of approximate scale thickness. The circular profiles of microbodies were traced with red ink. After completion of each transparency, it was superimposed upon the successive montage for near fit, and the corners were indicated to facilitate the positioning of the next sheet for the tracing of the same field from section-to-section. The transparencies can then be stacked upon a light box to scale and for closeness of fit employing the spherical microbodies as an internal index. Their circular profiles are concentrically stacked. Moreover, the spherical particles can be used for an internal determination of section thickness by dividing the profile diameter of the middle or equatorial serial section by the number of continuous serial sections in which the sphere appears.

Reconstructed volume is determined by the section area under the plastic transparent sheet, 279×356 mm, the magnification, the number of serial sections, and the section thickness. Extracellular space and karyoplasm must be subtracted from the total volume to yield reconstructed cytoplasmic volume.

Some mitochondria are completely contained in the reconstruction while others are fragmentary, extending beyond the six sides of the reconstructed volume. Therefore, to determine whether or not the fragments are like those that are complete, a statistical morphometric analysis of the fragments is necessary. The fragments are of further importance in determining the integral mitochondrial numbers and volumes per cytoplasmic volume.

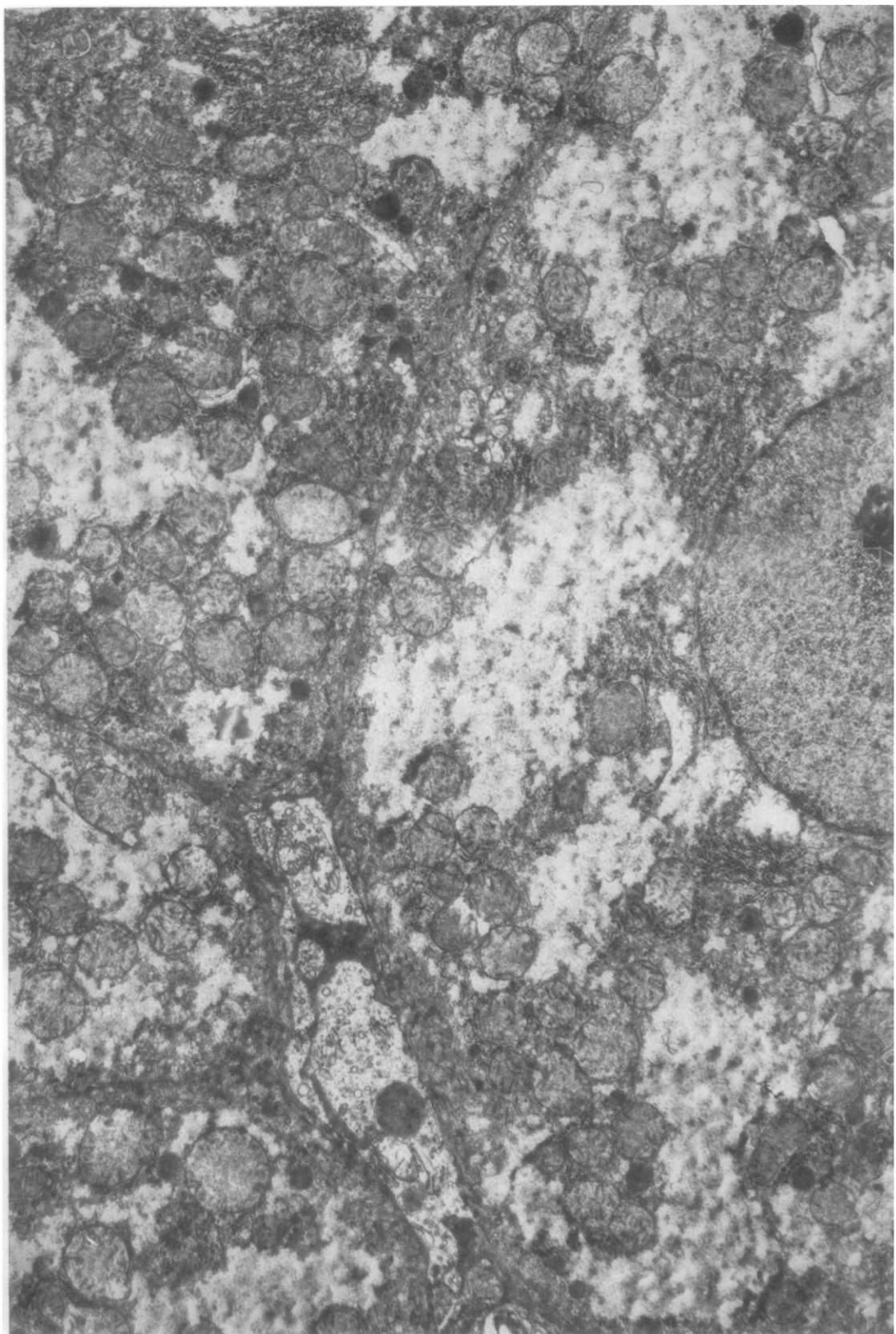
OBSERVATIONS

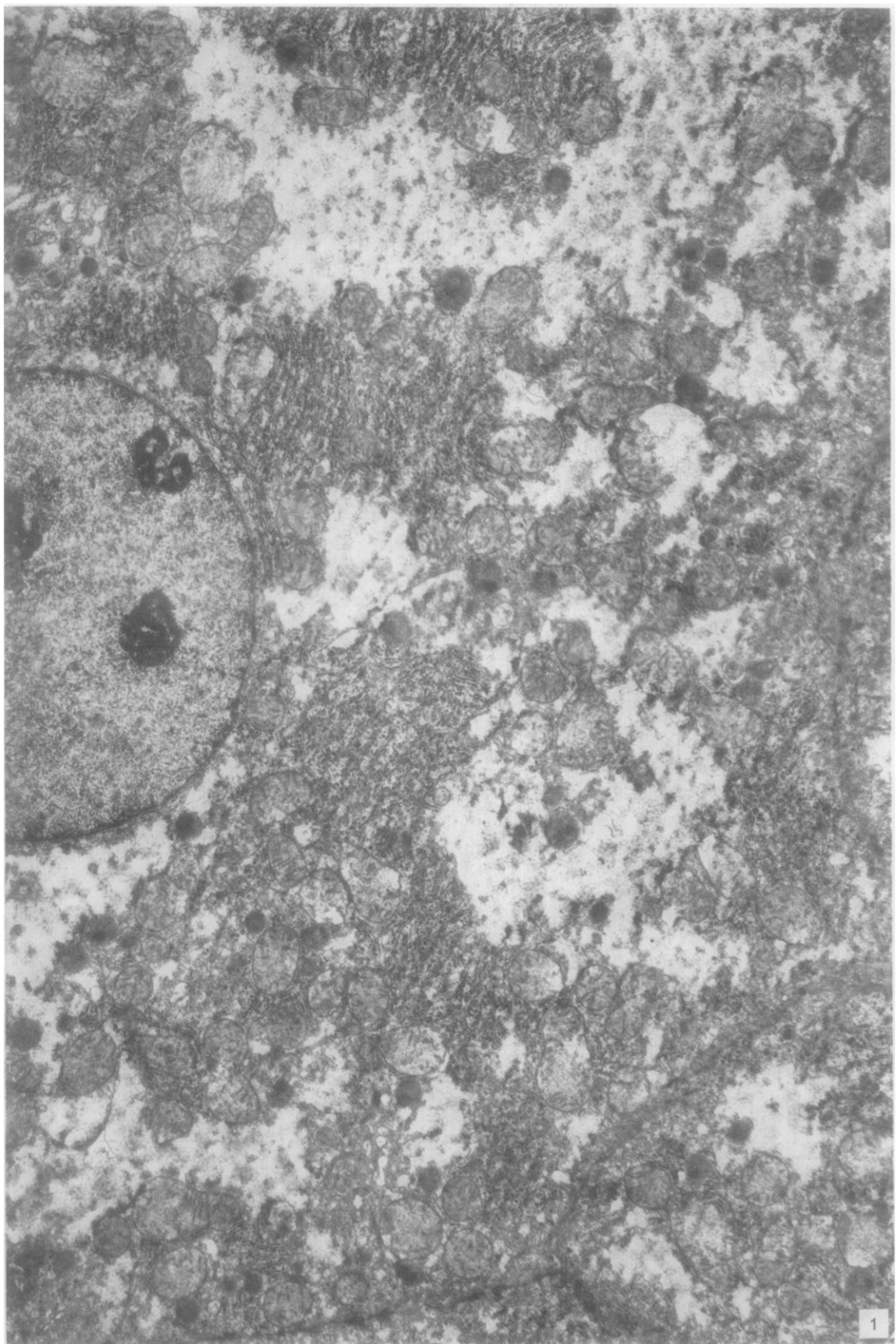
A variety of mitochondrial profile shapes are seen in random sections through rat liver (Fig. 1). They are circular, oval, rod-, crescent-, and dumbbell-shaped. Furthermore the limiting membrane may be in perpendicular, oblique, or tangential section. In the latter case it appears as a gray area in poor contrast with the surrounding ground substance, and when circular, indistinguishable from a tangential section through a microbody. When serial sections are available on either side of such a profile positive identification can be made with some confidence.

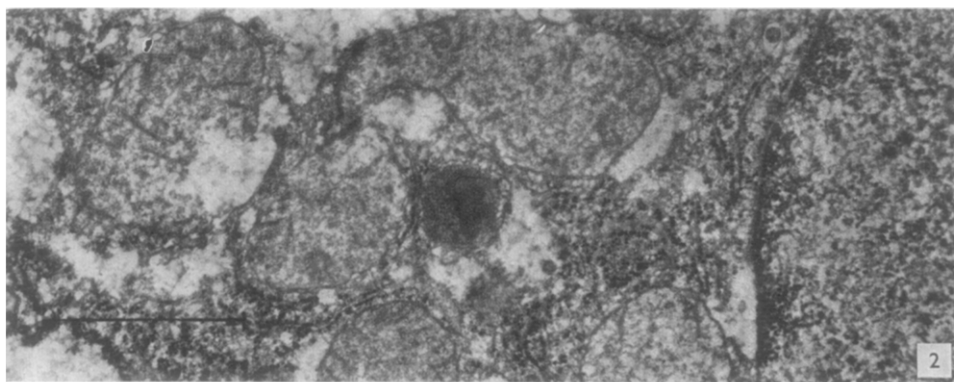
The reconstructions

The microbody is a spherical, membrane-bound particle about 400 nm in diameter (Fig. 2). The matrix is finely granular and some possess a denser medulla. Microbodies are distributed at random throughout the liver cytoplasm.

FIG. 1. A montage from L14 SS20(26) that can be considered as a random section through rat liver. Parts of karyoplasm and cytoplasm of an hepatocyte are seen. Note the variety of mitochondrial profile shapes, i.e., circular, oval, rod, crescent, and dumbbell shapes. Also note that limiting membranes are in perpendicular, oblique, and tangential section. ($\times 10\,500$.)







The following micrograph plates carry micron markers.
FIG. 2. The middle or equatorial serial section through a spherical microbody. Note the circular profile of the limiting membrane.

For use as internal indices for closeness of fit and determining section thickness, microbodies with nearly perfectly circular profiles in section were selected. Those lacking sphericity were excluded.

The circular diameter of the microbody measured in the middle or equatorial serial section divided by the number of serial sections in which the particle appears gives the section thickness. Mean section thicknesses for the three reconstructions appear in Table I. The mean section thicknesses determined internally are very close to the LKB-III Ultrotome settings of 300, 300, and 500 Å, respectively, with similar standard deviations of approximately 10 %. This is an indication of the reliability and precision of the instrument. In Table II find the resulting reconstructed cytoplasmic volumes and the total number of individual mitochondria, complete and fragmentary. Nearly 900 mitochondria were analyzed. The total reconstructed cytoplasmic volume was about 700 μm^3 derived in part from three hepatocytes.

Table I. *Section Thickness (Å)*

Reconstruction No.	LKB — III Setting	Determined Internally
L13 SS(47)	300	$302 \pm 28(10)^a$
L13 SS(40)	300	$304 \pm 38(10)$
L14 SS(26)	500	$474 \pm 39(24)$

^a Mean \pm standard deviation (sample size).

Table II. *Reconstructed Cytoplasmic Volumes and Number of Mitochondria*

Reconstruction No.	Reconstructed Cytoplasmic Volume (μm^3)	Number of Mitochondria Analyzed
L13 SS(47)	119	191
L13 SS(40)	220	336
L14 SS(26)	403	351
	742	878

The mitochondria

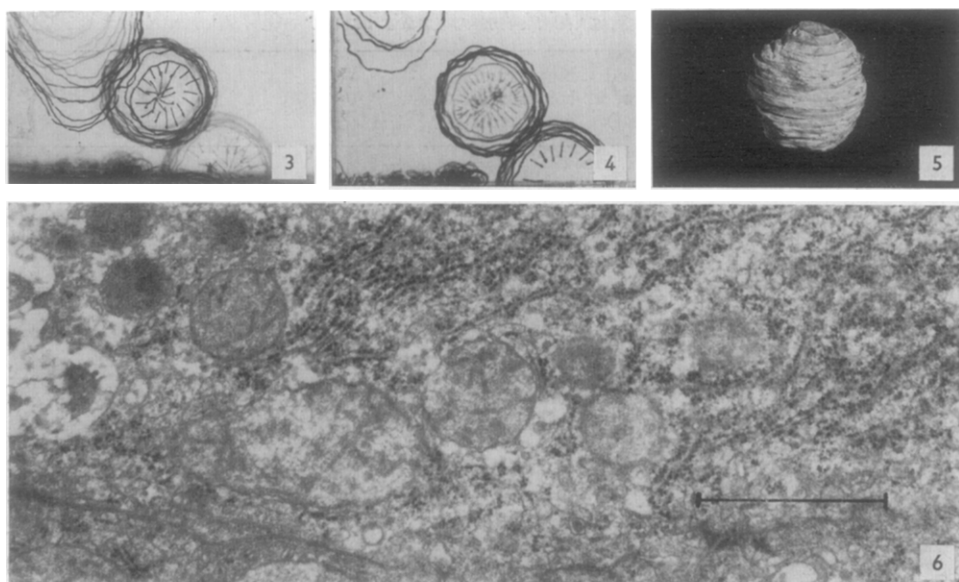
It is immediately obvious upon looking at the three-dimensional reconstructions of rat liver cytoplasm that the mitochondria are heterogeneous. The majority of the mitochondria are small rods distributed at random, and no plane through a rod can yield crescent or dumbbell profiles that are seen in random section.

Detailed analyses of those mitochondria that are complete within the reconstructions revealed two radically different mitochondrial populations: small cylindrical rods and larger V shapes, each arm of which is roughly cylindrical.

Rod-shaped mitochondria. The length of a cylindrical rod tilted at random to the plane of the section is determined by finding the hypotenuse of a right triangle whose other two sides are the projected length viewed from on top the reconstruction and the depth in serial sections times mean section thickness. The cylindrical diameter is equal to the profile minor axis measured in the middle serial section. In reconstruction L13 ss(47), the rods are 830 ± 220 nm (14) in length and 600 ± 110 nm (14) in cylindrical diameter. The Student's probability that the two means are statistically the same, i.e., that the mitochondria are really spherical rather than rod-shaped, is less than 0.01. The rod volume is about $0.18 \mu\text{m}^3$.

The rod dimensions in the other reconstruction from the same specimen, L13 ss(40), should be close as they are in a nearby hepatocyte and they are: 870 ± 210 nm (29) in length and 600 ± 90 nm (29) in cylindrical diameter. The probability that the means are statistically the same is less than 0.001. The rod volume is about $0.19 \mu\text{m}^3$. The probability that the rod lengths in L13 ss(47) and L13 ss(40) are the same is greater than 0.5. For the cylindrical diameters, the probability is greater than 0.9.

In another specimen, L14 ss(26), where the mitochondria would probably be expected to be of different sizes owing to the established linear size gradient (13), the rods are 930 ± 220 nm (30) in length and 660 ± 140 nm (39) in cylindrical diameter. The probability that the length is the same as the diameter is less than 0.001. Rod volume is about $0.24 \mu\text{m}^3$. The probabilities that the dimensions are the same in both



Figs. 3-6. Rod-shaped mitochondrion No. 194 at 0° tilt cut in cross section.

FIG. 3. India ink tracings on plastic transparent sheets of the profiles in all the serial sections through the complete rod-shaped mitochondrion No. 194 stacked to scale and for closeness of fit. The camera was focused on the top sheet using soft film so the sharpest, blackest lines are closest to the viewer's eyes and the broader, greyer lines farther away creating a three-dimensional effect.

FIG. 4. The same stack as in Fig. 3, but with the top half removed and the camera refocused on the profile tracing of the mid-serial section.

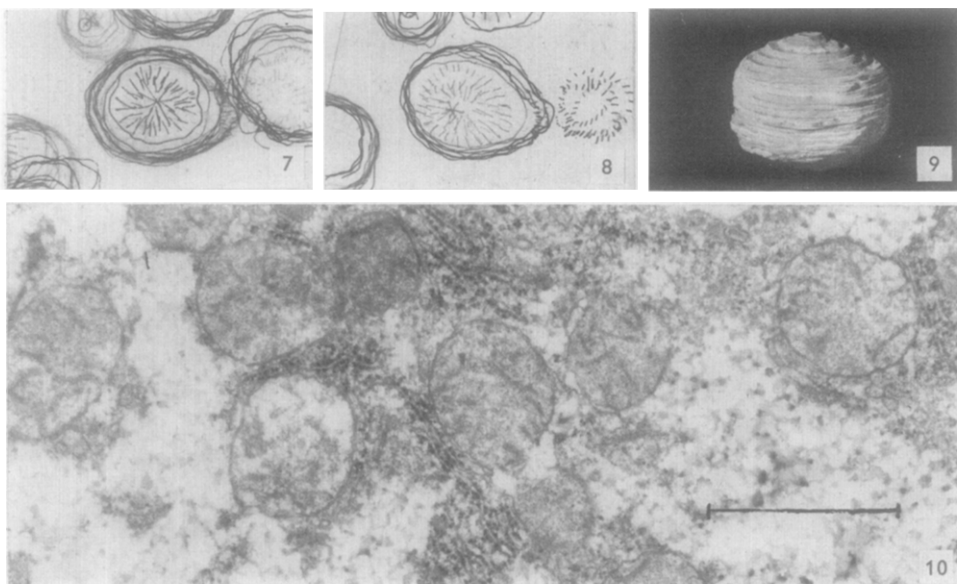
FIG. 5. The wooden model of rod-shaped mitochondrion No. 194.

FIG. 6. The electron micrograph of the mid-serial section through the rod-shaped mitochondrion No. 194. Note the circular mitochondrial profile in the center of the field.

specimens, L13 and L14, are less than 0.2 and 0.05, respectively, for length and diameter.

No mitochondrion, whether complete or fragmentary, was excluded from reconstruction. All profiles were counted and included for measurements and data analyses. However, since the mitochondria are distributed and tilted at random, those with more ideal orientation, i.e. 0°, 90°, or 180° tilt, were selected for illustrative purposes only.

Rod-shaped mitochondria that are fortuitously oriented in reconstruction are illustrated. Mitochondrion No. 194 is in 0° tilt and therefore was cut in cross section. The profile in each serial section is circular. A complete stack of the traced profiles on plastic transparent sheets is presented in Fig. 3. The camera was focused on the top plastic sheet so that the sharpest, blackest lines are closest to the reader's eyes and the broader, grayer lines are farther away, creating a three-dimensional illusion. Fig. 4 shows the same stack but with the top half removed putting the middle serial section



FIGS. 7-10. Rod-shaped mitochondrion No. 160 at 90° tilt cut longitudinally. Same format as in Figs. 3-6.

FIG. 7. The complete stack of plastic transparencies.

FIG. 8. The half stack with the top half of plastic transparencies removed so that the profile of the mid-serial section is in sharp focus.

FIG. 9. The wooden model.

FIG. 10. The electron micrograph of the mid-serial section. Note the oval mitochondrial profile in the center of the field. Unfortunately it was necessary to mount Fig. 10 at right angle orientation to Figs. 7-9.

in sharp focus. A scale wooden model is shown in Fig. 5. The electron micrograph of the middle serial section is presented in Fig. 6. A similar presentation is made of mitochondrion No. 160 in Figs. 7-10. Mitochondrion No. 160 is in 90° tilt and therefore cut longitudinally. Its profiles in serial sections are all oval.

Rod lengths and cylindrical diameters are unimodal in histograms for each specimen. Therefore rod-shaped mitochondria are a homogeneous class with regard to their stereomorphology.

V-shaped mitochondria. In L13 ss(47) the V arms are 1590 ± 210 nm(13) in length and 650 ± 100 nm(16) in cylindrical diameter. They are about $0.77 \mu\text{m}^3$ in volume. In another reconstruction from the same specimen, L13 ss(40), the V arms are 1590 ± 270 nm(19) in length and 580 ± 120 nm(35) in cylindrical diameter. The volume is about $0.64 \mu\text{m}^3$. The probabilities that the mean dimensions are statistically the same for the two reconstructions are greater than 0.9 for the lengths but only greater than 0.05 for the diameters.

In reconstruction L14 ss(26) from another specimen, slightly larger V shapes were found with arms 1860 ± 430 nm(17) long and 680 ± 130 nm(41) in cylindrical diameter. The volume is about $1.0 \mu\text{m}^3$. The Student's probabilities that the dimensions of the V-shaped mitochondria in specimen L13 and L14 are the same statistically are less than 0.01 for both lengths and diameters.

The mean angle formed by the two arms of the V-shaped mitochondria is $78 \pm 24^\circ$ (26).

For illustrative purposes only, V-shaped mitochondria with more ideal orientation were selected for presentation. Mitochondrion No. 82A in 90° tilt was sectioned longitudinally. The complete stack of profile tracings on plastic transparencies is shown in Fig. 11. The same stack with the top half of the serial sections removed is seen in Fig. 12. The camera was focused on the middle serial section. Therefore the crescent-shaped profile of the middle serial section is in sharp focus and Fig. 13 is the micrograph of the middle serial section. The wooden model is seen in Fig. 14.

Another V shape in 180° tilt, inverted in the reconstruction and cut in cross section is presented in Fig. 15 which is the complete stack of plastic transparent sheets. The wooden model is shown in Fig. 16. The profile seen in serial section No. 33 (Fig. 17) is rod-shaped and is a sectional plane through the vertex of the two arms. In serial section No. 30 (Fig. 18) the dumbbell profile is owing to the plane of section including the merging point of the two arms on their inside aspects. Were serial section No. 25 (Fig. 19) a random section, the likely spurious interpretation would be that the two discrete oval profiles represent two separate mitochondria. They are, however, profiles in section midway the lengths of two arms of the same V-shaped mitochondrion.

The wooden model of another V-shaped mitochondrion (No. 42) in 0° tilt and cut in cross section is presented in Fig. 20. V-arm lengths and cylindrical diameters are unimodal in histograms for each specimen. Therefore, V-shaped mitochondria are a homogeneous class in hepatocytes with regard to their stereomorphology.

The fragments

There are two radically different mitochondrial populations, rods and V shapes, among the mitochondria that are complete in the reconstructions. However, a morpho-

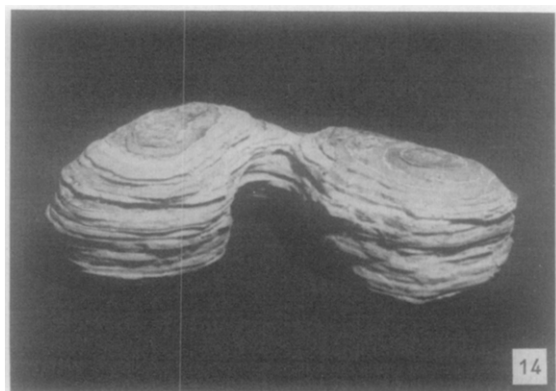
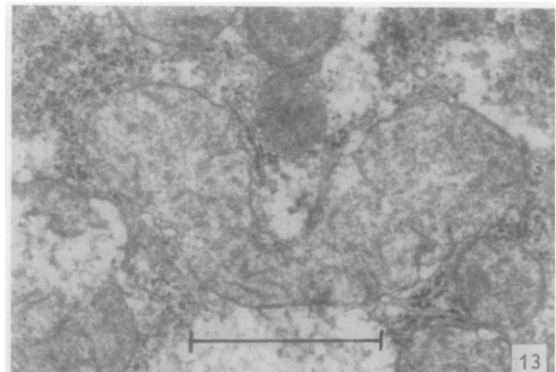
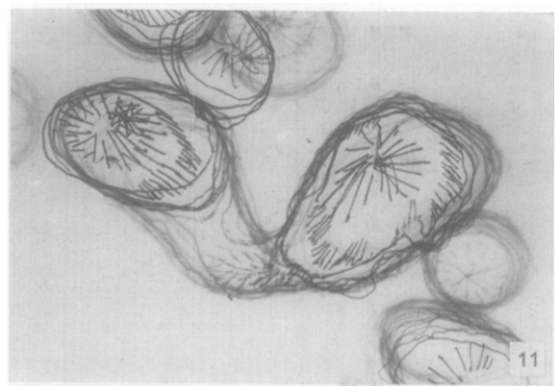
Figs. 11–14. V-shaped mitochondrion No. 82A at 90° tilt in longitudinal section. Similar format to Figs. 3–6 and 7–10.

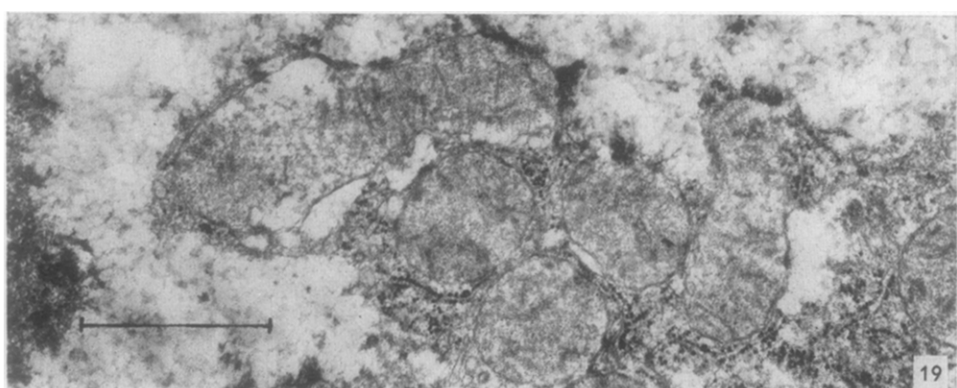
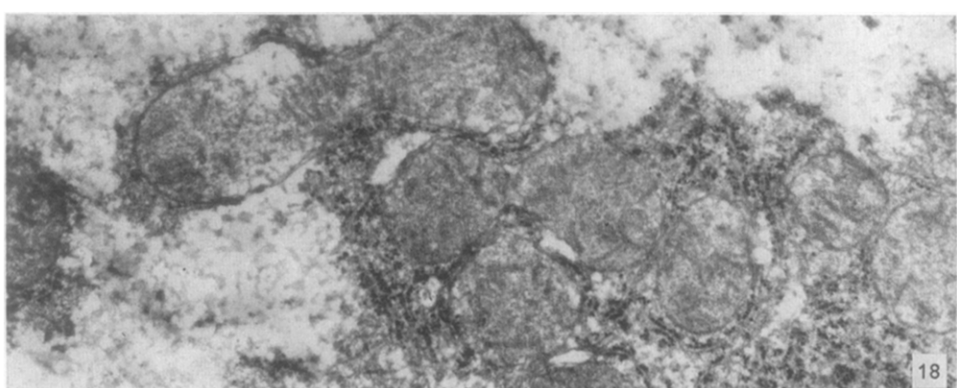
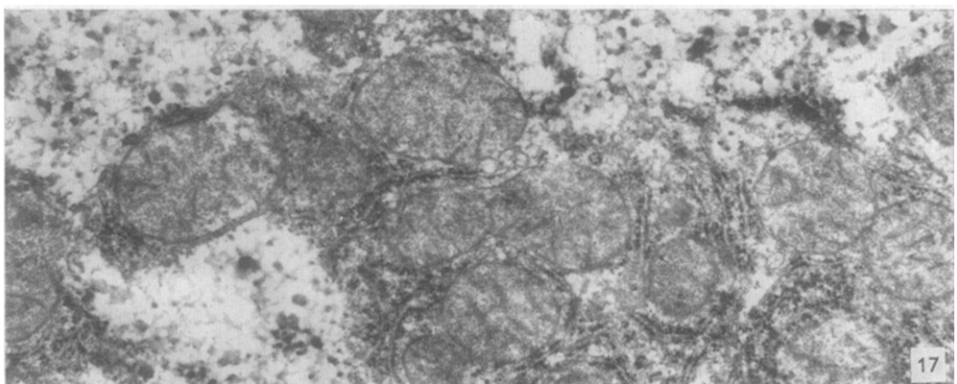
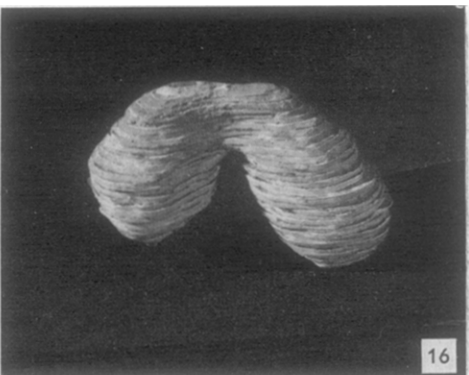
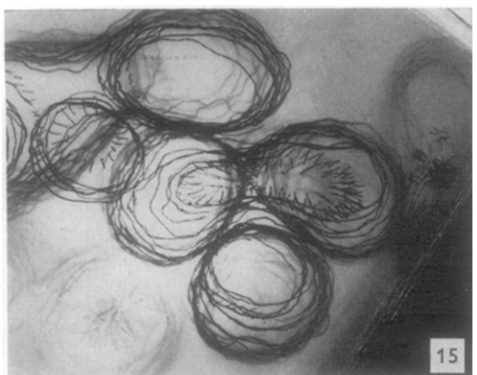
FIG. 11. The complete stack of plastic transparencies.

FIG. 12. The half stack with the top half of plastic transparencies removed so that the profile in the mid-serial section is in sharp focus.

FIG. 13. The electron micrograph of the mid-serial section. Note the crescent shape of the mitochondrial profile in the center of the field.

FIG. 14. The wooden model.





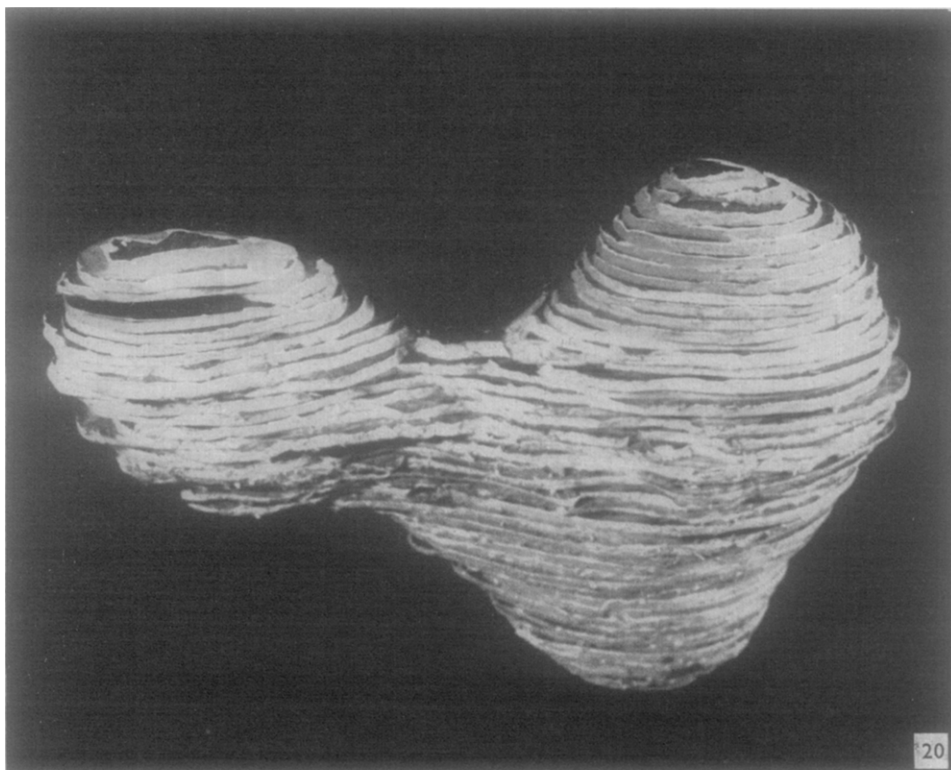


FIG. 20. The wooden model of mitochondrion No. 42 at 0° tilt cut in cross section. $\times 50\,000$.

metric analysis of the mitochondrial fragments that are incomplete, extending beyond the six sides of the reconstructions, is necessary to determine whether or not other sizes or shapes exist. If a mitochondrial population exists that is smaller than the rods,

Figs. 15–19. V-shaped mitochondrion No. 174 at 180° tilt (or inverted at 0° tilt) cut in cross section. Similar format as Figs. 3–6, 7–10, and 11–14.

FIG. 15. The complete stack of plastic transparencies.

FIG. 16. The wooden model.

FIG. 17. The electron micrograph of serial section No. 33 in a sectional plane midway between the vertex and the point of merger of the two V arms. Note the rod-shaped mitochondrial profile in the center of the field.

FIG. 18. The electron micrograph of serial section No. 30 through the point of merger of the two V arms. Note the dumbbell mitochondrial profile in the center of the field. The outermost component of the trilaminar limiting membrane is continuous about the whole profile; the innermost component is discontinuous, making two separate oval profiles.

FIG. 19. The electron micrograph of serial section No. 25 in a plane midway between the point of merger of the two V arms and the tips of each arm. Note the two separate oval mitochondrial profiles in the center of the field. Were this a micrograph of a random section, the two separate profiles would be spuriously interpreted as separate mitochondria.

Table III. *Rod Mean Depth (SS)*

Reconstruction No.	Observed (O)	Theoretical (T) (Range)	O/T (%)
L13 SS(47)	20 ± 5(14)	25 (20-27)	80
L13 SS(40)	24 ± 5(29)	26 (20-29)	92
L14 SS(26)	17 ± 4(39)	18 (14-20)	94

it would surely have been found unless the smaller mitochondria were very much less frequent. If a mitochondrial population exists that is larger than the V shapes, it might well be missed owing to the relative thinness of the reconstructions and the improbability of the larger mitochondria being at nearly 90° tilt in the reconstructions. Parameters that can be used to check this possibility are the mean profile major and minor axes in the middle serial sections through the particles and their distribution in histograms. The means and histograms of known mixtures of rods and V shapes can be compared to those of unknown fragments. The existence of larger mitochondria would produce larger means for the unknown fragments over the known mixture and would introduce a trail in their histograms toward longer major axes. Furthermore, in order to determine mitochondrial numbers and volumes per cytoplasmic volumes it is required that the fragments be included.

Since rods and V shapes have the same cylindrical diameters, a statistically significant difference of the mean minor axes in the middle serial section for a known mixture of rods and V shapes from unknown fragments would indicate the existence of mitochondria other than those known.

Mean depths. In order to ensure that major axes of fragment profiles not be oblique sections through the ends or edges of particles, which would decrease the means and distort the histograms, the mean depths of rods and V shapes are useful parameters. A fragment whose depth is less than half that for rods will not be included for major and minor axes measurement. Of course, they are included in determining total mitochondrial numbers and volumes.

The mean depths for rods in the three reconstructions are given in Table III. They are to be compared with the theoretical values for particles at 45° tilt. The difference

Table IV. *V Shape Average Depth (SS)*

Reconstruction No.	Observed Average (Range)	Theoretical Mean (Range)
L13 SS(47)	37 (27-47)	44 (22-53)
L13 SS(40)	27 (24-36)	43 (19-52)
L14 SS(26)	21 (20-22)	32 (14-39)

Table V. Number of Known Rod- and V-Shaped Mitochondria

Reconstruction No.	Rods (R)	V Shapes (V)	Ratio (R/V)
L13 SS(47)	14	7	2.0
L13 SS(40)	29	15	1.9
L14 SS(26)	39	17	2.3

between the theoretical and observed value for rods is an indication of the percent of section profiles missed owing to the poor contrast of tangential top and bottom pieces. The facility for identifying tangential pieces improved temporally from the first to the third reconstruction from 80 to 94 %.

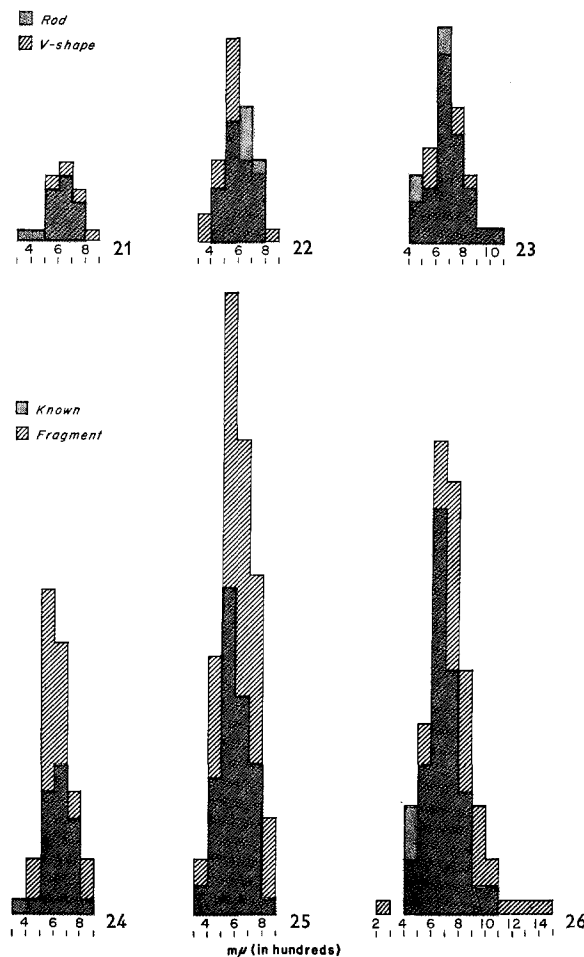
Mean depths for the V shapes in the three reconstructions are given in Table IV. The differences between theoretical and observed values reflect the low probability of large V shapes being complete in the reconstructions if in less than 45° tilt owing to the relative shallowness of the reconstruction.

Frequency. The numbers of known rod- and V-shaped mitochondria in the three reconstructions are given in Table V. In each case the ratio of rods: V shapes is about 2:1. Therefore, the frequency of rods among the total known mitochondria is about 2:3 and that for V shapes is about 1:3. As each V shape has two arms, the ratio of rods: V arms is about 1:1.

Mean minor axes. The minor axes in the middle serial section of a cylinder tilted at random is the same regardless of the angle of tilt. It is equal to the cylindrical diameter. Both the rod- and V-shaped mitochondria have cylindrical components. The cylindrical diameters of rods and V arms are statistically the same in a given reconstruction. A comparison of the mean minor axes in mid-serial section of a mixture of known rods and V shapes with the mean minor axis in near mid-serial section of the fragments will detect a class of mitochondria with a diameter different from that of the rod and V shapes. The mean minor axes in mid-serial section for mixtures of known rod and V shapes and the mean minor axes in near mid-serial section of fragments for the three reconstructions are presented in Table VI. The Student's pro-

Table VI. Mean Minor Axis in Mid-Serial Section (nm)

Reconstruction No.	Known Mixture of Rod + V Shapes	Fragments
L13 SS(47)	$630 \pm 100(30)$	$630 \pm 100(61)$
L13 SS(40)	$590 \pm 100(64)$	$610 \pm 110(139)$
L14 SS(26)	$670 \pm 130(80)$	$740 \pm 170(120)$



FIGS. 21-32. Histograms.

FIGS. 21-23. Comparison of profile minor axes in the mid serial sections of complete and known rod-shaped vs V-shaped mitochondria.

FIG. 21. Reconstruction L13 ss (47).

FIG. 22. Reconstruction L13 ss (40).

FIG. 23. Reconstruction L14 ss (26).

FIGS. 24-26. Comparison of profile minor axes in the mid-serial sections of known mixtures of rod- and V-shaped mitochondria vs the profile minor axes in the estimated mid-serial sections of unknown fragmentary mitochondria.

FIG. 24. Reconstruction L13 ss (47).

FIG. 25. Reconstruction L13 ss (40).

FIG. 26. Reconstruction L14 ss (26).

Table VII. Mean Major Axis in Mid-Serial Section (nm)

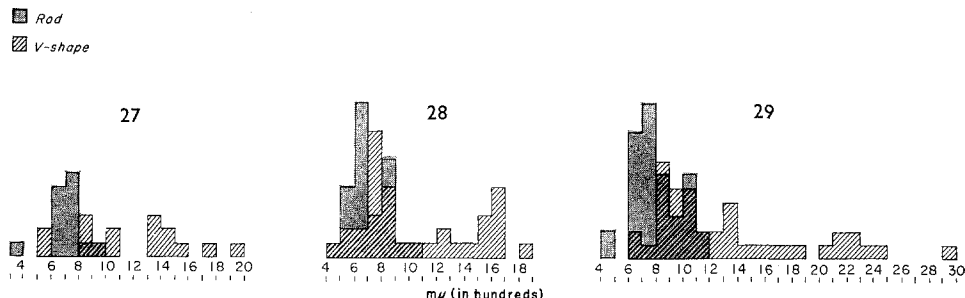
Reconstruction	Rods	V Shapes
L13 SS(47)	$700 \pm 124(14)$	$1\ 180 \pm 410(16)$
L13 SS(40)	$700 \pm 140(29)$	$1\ 060 \pm 400(35)$
L14 SS(26)	$810 \pm 170(39)$	$1\ 340 \pm 570(41)$

bility that the means for the known mixture and the fragments is the same is greater than 0.9 for L13 ss(47) and greater than 0.5 for L13 ss(40). However, the difference of the means for L14 ss(26) is significant at the 0.001 level. In histograms, the distribution of minor axes is unimodal in all cases (Figs. 21-26).

Mean major axes. The range of values for profile major axes in the middle serial section through a cylindrical rod is from the cylindrical diameter at 0° tilt to the rod length at 90° tilt. The same is true for individual V arms. The mean value for particles at random tilt coincide with the profile major axis in mid-serial section at 45° tilt. The standard deviation is a function of the range. The mean major axes in mid serial section for rod and V shapes are given in Table VII. The probability that the differences in the means for rod and V shapes for the three reconstructions are insignificant is less than 0.001.

Histograms of the major axis in mid-serial section for rods are unimodal, while for V shapes they are bimodal (Figs. 27-29). The bimodality is owing to the fact that the major axis in one V arm and the major axis in the other arm of the same V shape are not independent events.

The mean major axes and standard deviations in mid-serial section for known mixtures of rod- and V-shaped mitochondria and the mean major axes and standard



Figs. 27-29. Comparison of profile major axes in the mid-serial sections of complete and known rod-shaped vs V-shaped mitochondria.

FIG. 27. Reconstruction L13 ss (47).

FIG. 28. Reconstruction L13 ss (40).

FIG. 29. Reconstruction L14 ss (26).

Table VIII. Mean Major Axis in Mid-Serial Section (nm)

Reconstruction No.	Known Mixture of Rod- + V Shapes	Fragments ^a
L13 SS(47)	960±390(30)	900±290(61)
L13 SS(40)	900±360(64)	800±280(138)
L14 SS(26)	1 080±500(80)	1 040±400(120)

^a Estimated mid-serial section

deviations in near mid-serial section for fragments in the three reconstructions are presented in Table VIII. The probabilities that the mean values for known mixtures and fragments are the same statistically are greater than 0.2, 0.5, and 0.5, respectively, for the three reconstructions. There is insufficient evidence in the histograms of these data (Figs. 30–32) to suggest the existence of a mitochondrial population that is larger than the V shapes. The shapes of the bimodal histograms of the fragments are similar to those of the known mixtures of rods and V shapes. The ranges of values are nearly the same for both. There are no trails of longer values among the fragments.

The model

Among the complete and known mitochondria in the reconstructions of rat hepatocytes, there are two populations of mitochondria: rod and V shapes in a 2:1 ratio. Analyses of the fragments failed to detect any dissimilar mitochondria and are consistent with the model that there are two and probably only two populations of hepatocyte mitochondria. Employing this model, total mitochondrial numbers and volumes per cytoplasmic volume can be determined and checks made on the model.

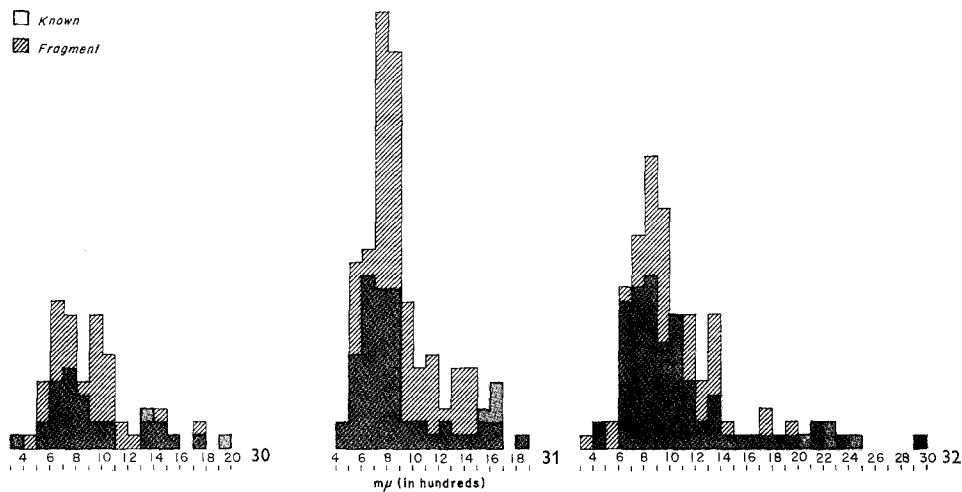
Mitochondrial number per cytoplasmic volume. The integral number of mitochondria contained in the total number of unknown fragment profiles in the reconstruction is a function of the frequencies of complete and known rod- and V-shaped mitochondria and their respective mean depths expressed by Eqs. (1) and (2):

$$N = R d + 2 V D \quad (1)$$

$$r/v = R/V \quad (2)$$

where N =total number of unknown fragment profiles; R =integral number of rods represented in the fragments; d =mean depth in serial sections of complete rods; V =integral number of V shapes represented in the fragments; D =mean depth in serial sections of known V shapes; r =number of complete rods; and v =integral number of known V shapes. Solving (Eq. 2) for V :

$$V = (v R)/r \quad (3)$$



Figs. 30-32. Comparison of profile major axes in the mid-serial sections of known mixtures of rod- and V-shaped mitochondria vs the profile major axes in the estimated mid-serial sections of unknown fragmentary mitochondria.

FIG. 30. Reconstruction L13 ss (47).

FIG. 31. Reconstruction L13 ss (40).

FIG. 32. Reconstruction L14 ss (26).

and substituting Eq. (3) in eq. (1) and solving for R gives:

$$R = N/[d + (2 Dv)/r]$$

Solving Eq. (2) for R :

$$R = (r V)/v \quad (4)$$

and substituting Eq. (4) in Eq. (1) and solving for V gives:

$$V = N/[(dr)/v + 2D]$$

The factor 2 is necessary as each V shape has two arms. The total integral number of rods (R_T) is:

$$R_T = r + R$$

and the total integral number of V shapes (V_T) is: $V_T = v + V$

The total number of fragment profiles found was 1456.0 in L13 ss(47), 3984.5 in L13 ss(40), and 2266.5 in L14 ss(26). For the three reconstructions the total integral numbers of mitochondria as distributed among rod and V shapes are given in Table

Table IX. *Integral Number of Mitochondria*

Reconstruction	Rods	V Shapes	Total
L13 SS(47)	39	20	59
L13 SS(40)	90	47	137
L14 SS(26)	92	40	132

IX. Dividing the total integral numbers of mitochondria by the reconstructed cytoplasmic volumes yields the mean numbers of mitochondria per cubic micrometer. These values as given in Table X are seen to vary widely among the three reconstructions.

Mitochondrial volumes per cytoplasmic volume. The numbers of rod- and V-shaped mitochondria times their respective volumes yields the total mitochondrial volume for each reconstruction. The total mitochondrial volumes divided by the reconstructed cytoplasmic volumes give the mitochondrial volumes per cytoplasmic volumes. These values expressed in percents are given in Table X for the three reconstructions. While mitochondrial numbers per cytoplasmic volumes vary widely, mitochondrial volumes per cytoplasmic volumes are relatively close in values for the three reconstructions, i.e., about 19 %. This suggests that where in the size gradient the mitochondria are smaller, they are more numerous and where they are larger, they are less numerous proportionately.

Mitochondrial area per cytoplasmic area. The total profile area in a plane through random particles in space is equal to the total volume occupied by the particles in that space. As a check of the model, the total mitochondrial areas as a percent of the cytoplasmic areas in the first serial section of each reconstruction were determined. These values are relatively close for the three reconstructions at about 20 %, and individually they correlate well with the values for mitochondrial volumes per cytoplasmic volumes as presented in Table X.

Table X. *Mitochondrial Number, Volume and Area vs Cytoplasmic Volume and Area*

Reconstruction No.	Mean Number Mitochondria per Cytoplasmic Volume ($m/\mu\text{m}^3$)	Mitochondrial Volume per Cytoplasmic Volume (%)	Mitochondrial Area per Cytoplasmic Area (%)
L13 SS(47)	0.50	19	22
L13 SS(40)	0.62	21	21
L14 SS(26)	0.33	16	17

Table XI. *Minor Axis Compared with Cylindrical Diameter*

Reconstruction No.	Mean Random Minor Axis (δ) (nm)	Calculated Mean Cylindrical Diameter (Δ) ^a (nm)	Error Δ vs m^b (%)
L13 SS(47)	550	630	0.6
L13 SS(40)	500	570	3.1
L14 SS(26)	650	750	11.8

^a $\Delta = 2\delta/\sqrt{3}$.^b m = mean minor axis in mid-serial section or cylindrical diameter.

Mean random minor axis as a function of mean minor axis in mid-serial section. The average profile diameter of all the circular profiles seen in n planes through a sphere is equal to the profile diameter in the plane at one-half the radius ($r/2$) distance from the equatorial plane. The true equatorial diameter (Δ) is related to the profile diameter (δ) at $r/2$ as follows:

$$\Delta = 2\delta/\sqrt{3} \quad (5)$$

Both the rod- and V-shaped mitochondria have cylindrical components and the cylindrical diameters of each are approximately equal. The minor axis of the profile in the mid-serial section of a cylindrical mitochondrion at random tilt is equal to the cylindrical diameter. In a section through random cylindrical mitochondria, the mean random minor axis is related to the true cylindrical diameter in the same way as expressed in Eq. (5) by analogy.

As a further check on the model, the minor axes of all the mitochondrial profiles in the first serial section of each reconstruction were measured. The mean random minor axes adjusted by the factor $2/\sqrt{3}$ from Eq. (5) compare favorably with the mean minor axes in the mid-serial section or the mean cylindrical diameters (Table XI) for the three reconstructions.

The gradient

In a montage of 35 plates of a large face section through L15 comprising more than 20 hepatocytes, the mitochondrial mean minor axes were found to differ from cell to cell. While the sectional plane did not coincide precisely with the linear size gradient reported by Loud (13), in six hepatocyte linear array from an arteriole to the section edge over a length of about 60 μm , the mitochondrial mean minor axes for each cell did approximate a linear gradient. The data are given in Table XII.

Table XII

Hepatocyte Number (L15)	Distance from Origin (μm)	Mitochondrial Mean Minor Axis (nm)
(Arteriole)	0	—
6	8	830 \pm 230(20)
4	24	820 \pm 190(20)
3	32	780 \pm 210(20)
20	34	750 \pm 180(20)
2	38	740 \pm 170(20)
1	50	700 \pm 170(20)
(Section edge)	55	—

DISCUSSION

Among the mitochondria that are complete in the three-dimensional reconstructions from serial sections through rat liver, two different morphological classes were found: rod and V shapes. They differ in their stereomorphological shape and size, but not in their internal fine structure at the level of resolution of this study. The known rod and V shapes are distributed at random in a 2:1 ratio within the hepatocyte.

Morphometric analyses of the fragmentary mitochondria extending beyond the six sides of the reconstructions failed to detect classes other than rod and V shapes. None was detected with significantly different cylindrical diameter on the basis of comparing profile minor axes in the estimated mid serial sections of fragments to profile minor axes in the mid serial sections through the complete and known mitochondria. A similar comparison of profile major axes of fragments and known mixtures of rods and V shapes revealed neither smaller nor larger mitochondria.

The data from the complete mitochondria and the fragment analyses are consistent with the model that there are two, and probably only two, radically different mitochondrial populations, rod and V shapes, distributed at random in a 2:1 ratio in the rat hepatocyte. The model accounts for all the variety of profile shapes seen in random section. Mitochondrial area per cytoplasmic area in random section fits well with the mitochondrial volume per cytoplasmic volume as determined on the basis of the model. In random section through cylinders, the mean minor axis of the profiles will coincide with the profile minor axis in a plane at one half the cylindrical radius. The mean minor axis of mitochondrial profiles compared favorably with the cylindrical diameters when corrected accordingly on the basis of the model, albeit the error for L14(26) is 12%.

Mitochondrial size gradient. The difference in sizes of rod- and V-shaped mitochondria within a single hepatocyte is not to be confused with the linear size gradient across

the lobule, from the central vein to the hepatic triad, as established by Loud (13). If these data from three hepatocytes prove general, both rod- and V-shaped mitochondria are arrayed in a size gradient with their dimensions relative to each other remaining proportionately constant within a given hepatocyte.

However, where the mitochondria are smaller, they appear more numerous and where larger, fewer, maintaining relatively constant mitochondrial volume per cytoplasmic volume. As there is a gradient of oxygen tension from the hepatic arteriole in the triad to the central vein, one may speculate that the mitochondrial size gradient is a function of oxygen tension. As the mitochondrial use of oxygen is internal, it crosses the limiting membrane. This is a surface function. As mitochondrial surface area is a square function and mass (volume) is a cube function, the smaller the mitochondrion, the greater is the surface-to-mass ratio. In relatively oxygen-poor regions nearer the central vein, the more numerous, smaller mitochondria have a greater total surface area over which to compete for the rarer oxygen.

The single observation made here of a size gradient over six cells on the basis of a large face section including at least 20 hepatocytes can not be intended as confirmation of the size gradient demonstrated by Loud (13). Rather, it suggests that there may be mitochondrial size differences from cell-to-cell in the gradient. In the study by Loud, measurements were made in defined areas of liver tissue comprising parts of several hepatocytes.

Enzyme activity heterogeneity. By means of zonal centrifugation of isolated rat liver mitochondria ornithine transcarbamolase and aminotransferase have been shown to be associated with larger and smaller particles, respectively. These enzymes may be components of the larger V-shaped and the smaller rod-shaped mitochondria, respectively, rather than a function of the size gradient. This interpretation is consistent with their uniform histochemical distribution across the liver lobule. Other enzyme differences may well be discovered. However, it appears that the enzymes of oxidative phosphorylation are components of both size classes (11, 17, 18, 25, 28). This being interpreted in light of the molecular micellar model for mitochondrial membranes of Sjöstrand (20, 21) and Sjöstrand and Barajas (22) is consistent with the notion that the two radically different mitochondrial shapes in rat liver are owing to their different protein compositions. This speculation may be analogous to the radically different shapes of normal red blood cells and sickle cells owing to a single amino acid difference in their respective hemoglobins (10).

Artifacts of isolation. Except in the fixation study of Butler and Judah (6), isolated hepatic mitochondria from cell fractions do not resemble *in situ* profiles in electron micrographs. Schuel et al. (17, 18 and in preparation) have partially separated two morphological classes of mitochondria, each in a linear size gradient by means of zonal centrifugation in a sucrose density gradient. Cytochrome oxidase activity was

bimodally distributed being associated with both classes. However, the morphological differences of the two classes, aside from size, were the condensed matrix and orthodox configurations defined by Hackenbrock (9). Rather than an explanation owing to physiological state, it may be interpreted as differing artifactual responses of radically different mitochondria to similar isolation procedures.

Bahr and Zeitler (1) found two morphological classes in a 1:1 ratio, each in a linear size gradient, in isolated mitochondria from rat liver. Rather than being a reproductive cycle, these data may now be understood in light of artifacts of isolation, the linear size gradient of Loud (13) and the present work. The spheres, the diameters of which were half the length of rods, may have been derived from rod-shaped mitochondria, whose length is half that of the V arms, by slight swelling. The rods were possibly derived from V-shaped mitochondria by tearing apart the two arms by shearing. The ratio of rod- to V-shaped mitochondria is two-to-one. The ratio of rods to V arms is one-to-one.

In 1953, Laird et al. (12) separated isolated rat liver mitochondria into two layers by means of differential centrifugation. Both layers exhibited succinoxidase activity. In a correlated electron microscopic study, they found small rod-shaped particles in the top layer and larger rod-shaped and V-shaped particles in the bottom layer.

The biconcave disk model. On the basis of 30 serial sections 600–1 200 Å thick, through an incomplete rat liver mitochondrion, Stempac (23, 24) proposed a biconcave disk model, similar in shape to red blood cells. The limited reconstruction and the range of section thicknesses make it difficult to interpret in light of the present model.

Spurious three-dimensional interpretations from two-dimensional micrographs. Finally, one ought to be mindful of space in making interpretations from two dimensional pictures of random sections (7). A rod-shaped profile need not indicate a rod-shaped mitochondrion as is learned from Fig. 17. A dumbbell mitochondrial profile need not indicate a dividing mitochondrion (8) as is learned from Fig. 18. Two separate profiles need not indicate two discrete mitochondria but may indeed be profiles of the same mitochondrion as is learned in Fig. 19. Furthermore, at present there is no reason to believe from these morphological data or from available enzymological data, that one population differentiates into the other or is derived from the other.

Innovative and imaginative artistic, photographic, analytical, and technical assistances were contributed by Messrs. V. Stephen Piro, W. Terranova, C. Bergengren, P. Morin, R. Piro, and F. Partington Wedel. The histograms were drawn by Mr. Charles Mills and photographed by Mr E. G. Hertling, of Medical Illustration. Mrs Esther Cinman typed the manuscript.

The author is grateful to Dr Philip Person, Chief, Special Research Laboratory for Oral Tissue Metabolism, Veterans Administration Hospital, Brooklyn, New York for generously providing criticism, support, and space; and Dr Charles Lieber, Chief, Liver Disease and

Nutrition, Veterans Administration Hospital, Bronx, New York, for stimulating interest in liver and specimens.

The work was done in part at Mount Sinai School of Medicine.

Financial support in part was provided by National Science Foundation Grant No. GB-29759 and Friends of Medical Science Research, Baltimore, Maryland.

REFERENCES

1. BAHR, G. F. and ZEITLER, E., *J. Cell Biol.* **15**, 489 (1962).
2. BERGER, E. R., *J. Ultrastruct. Res.* **11**, 90 (1964).
3. —— *J. Cell Biol.* **35**, 11 A (1967).
4. —— *ibid.* **39**, 12a (1968).
5. BRODY, I., *J. Ultrastruct. Res.* **2**, 482 (1959).
6. BUTLER, W. H. and JUDAH, J. D., *J. Cell Biol.* **44**, 278 (1970).
7. ELIAS, H., *Science* **174**, 993 (1971).
8. FAWCETT, D. W., *J. Nat. Cancer Inst.* **15**, 1475 (1955).
9. HACKENBROCK, C. R., *J. Cell Biol.* **30**, 269 (1966).
10. —— *ibid.* **37**, 345 (1968).
11. INGRAM, V. M., *Nature (London)* **180**, 326 (1957).
12. LAIRD, A. K., NYGAARD, O., RIS, H. and BARTON, A. D., *Exp. Cell Res.* **5**, 147 (1953).
13. LOUD, A. V., *J. Cell Biol.* **37**, 27 (1968).
14. NOVIKOFF, A. B. and SHIN, W. Y., *J. Microsc. (Paris)* **3**, 187 (1964).
15. RYTER, A. and KELLENBERGER, E., *J. Ultrastruct. Res.* **2**, 200 (1958).
16. SABATINI, D. D., BENSCH, K. and BARRNETT, R. J., *J. Cell Biol.* **17**, 19 (1963).
17. SCHUEL, H. and BERGER, E. R., *Biophys. Soc. Abstr., 16th Annu. Meeting, Toronto*, p. 133a (1972).
18. SCHUEL, H., BERGER, E. R., WILSON, J. R. and SCHUEL, R., *J. Cell Biol.* **43**, 125a (1969).
19. SJÖSTRAND, F. S., *J. Ultrastruct. Res.* **2**, 122 (1958).
20. —— *Protides Biol. Fluids Proc. Colloq.* **15**, 15 (1967).
21. —— in RICHTER, G. W. and SCARPELLI, D. G. (Eds.), *Cell Membranes. Biological and Pathological Aspects*, pp. 1-29. Williams & Wilkins, Baltimore, Maryland, 1971.
22. SJÖSTRAND, F. S. and BARAJAS, L., *J. Ultrastruct. Res.* **32**, 293 (1970).
23. STEMPAK, J., *Anat. Rec.* **151**, 420 (1965).
24. —— *J. Ultrastruct. Res.* **18**, 619 (1967).
25. SWICK, R. W., STANGE, J. L., NANCE, S. L. and THOMSON, J. F., *Biochemistry* **6**, 737 (1967).
26. SWICK, R. W., TOLLAKSEN, S. L., NANCE, S. L. and THOMSON, J. F., *Arch. Biochem. Biophys.* **136**, 212 (1970).
27. VENABLE, J. H. and COGGESHALL, R., *J. Cell Biol.* **25**, 407 (1970).
28. WONG, D. T., VAN FRANK, R. M. and HORNG, J.-S., *Life Sci. Pt. 2* **9**, 1013 (1970).